Shmt1 and de novo thymidylate biosynthesis underlie folate-responsive neural tube defects in mice[1–4]

Anna E Beaudin, Elena V Abarinov, Drew M Noden, Cheryll A Perry, Stephanie Chu, Sally P Stabler, Robert H Allen, and Patrick J Stover

ABSTRACT

Background: Folic acid supplementation prevents the occurrence and recurrence of neural tube defects (NTDs), but the causal metabolic pathways underlying folic acid–responsive NTDs have not been established. Serine hydroxymethyltransferase (SHMT1) partitions folate-derived one-carbon units to thymidylate biosynthesis at the expense of cellular methylation, and therefore SHMT1-deficient mice are a model to investigate the metabolic origin of folate-associated pathologies.

Objectives: We examined whether genetic disruption of the *Shmt1* gene in mice induces NTDs in response to maternal folate and choline deficiency and whether a corresponding disruption in de novo thymidylate biosynthesis underlies NTD pathogenesis.

Design: *Shmt1* wild-type, $Shmt1^{+/-}$, and $Shmt1^{-/-}$ mice fed either folate- and choline-sufficient or folate- and choline-deficient diets were bred, and litters were examined for the presence of NTDs. Biomarkers of impaired folate metabolism were measured in the dams. In addition, the effect of *Shmt1* disruption on NTD incidence was investigated in $Pax3^{Sp}$ mice, an established folate-responsive NTD mouse model.

Results: $Shmt1^{+/-}$ and $Shmt1^{-/-}$ embryos exhibited exencephaly in response to maternal folate and choline deficiency. *Shmt1* disruption on the $Pax3^{Sp}$ background exacerbated NTD frequency and severity. *Pax3* disruption impaired de novo thymidylate and purine biosynthesis and altered amounts of SHMT1 and thymidylate synthase protein.

Conclusions: SHMT1 is the only folate-metabolizing enzyme that has been shown to affect neural tube closure in mice by directly inhibiting folate metabolism. These results provide evidence that disruption of *Shmt1* expression causes NTDs by impairing thymidylate biosynthesis and shows that changes in the expression of genes that encode folate-dependent enzymes may be key determinates of NTD risk. *Am J Clin Nutr* 2011;93:789–98.

INTRODUCTION

During embryogenesis, the neuroepithelium bends and fuses to form the embryonic neural tube through the process of neurulation. Failure of neurulation results in a spectrum of developmental anomalies collectively referred to as *neural tube closure defects* (NTDs). Worldwide prevalence of human NTDs ranges from <1–30 per 10,000 births (1). One of the strongest environmental determinants of NTD risk is low maternal folate status (2), which interacts with specific gene variants to confer NTD risk (3, 4). Maternal folic acid supplementation reduces both NTD occurrence and recurrence (5, 6). However, the folate-dependent metabolic pathway or pathways that affect neural tube closure are unknown.

Folates function as enzyme cofactors that carry one-carbon units for a network of anabolic pathways collectively known as one-carbon metabolism (OCM; **Figure 1**). OCM is essential for de novo purine and thymidylate (dTMP) synthesis and for the remethylation of homocysteine to methionine, which can be adenosylated to form the universal methyl donor *S*-adenosylmethionine (AdoMet) (Figure 1). OCM can be impaired by genetic variation or nutrient deficiencies or both, which can simultaneously disrupt de novo nucleotide biosynthesis and AdoMet synthesis, resulting in reduced proliferative capacity, increased uracil in DNA, elevated plasma homocysteine, and reduced cellular methylation (7). It is not known which of these impairments ultimately contributes to NTD pathogenesis.

Responsiveness to maternal folate supplementation has been determined in only a few of the 150 mouse models (8) that exhibit NTDs (9–12), and of those NTD models that respond to exogenous folic acid only the *Splotch* mutant ($Pax3^{Sp}$) has shown impairment in OCM. Homozygous *Splotch* embryos exhibit fully penetrant spina bifida and impaired de novo thymidylate biosynthesis (10). NTDs in the *Splotch* mutant can be rescued with supplemental dietary folic acid or thymidine, indicating that folic acid prevents NTDs by rescuing de novo thymidylate synthesis in this mouse model (9, 10). However, *Pax3* has not been linked to human NTD pathogenesis in epidemiologic studies (13, 14).

The thymidylate biosynthesis pathway is composed of 3 enzymes that function in the cytoplasm and the nucleus: thy-

[1] From the Division of Nutritional Sciences (AEB, EVA, CAP, SC, and PJS), and the Department of Biomedical Sciences, College of Veterinary Medicine (DMN), Cornell University, Ithaca, NY; and the Department of Medicine and Division of Hematology, University of Colorado Health Sciences Center, Denver, CO (SPS and RHA).

[2] Supported by Public Health Service grant HD059120 to PJS and T32-DK007158 to AEB.

[3] Present address for AEB: Department of Biomolecular Engineering, University of California, Santa Cruz, Santa Cruz, CA 95064.

[4] Address correspondence to PJ Stover, Division of Nutritional Sciences, 315 Savage Hall, Cornell University, Ithaca, NY 14853. E-mail: pjs13@cornell.edu.

Received August 20, 2010. Accepted for publication January 25, 2011.

First published online February 23, 2011; doi: 10.3945/ajcn.110.002766.

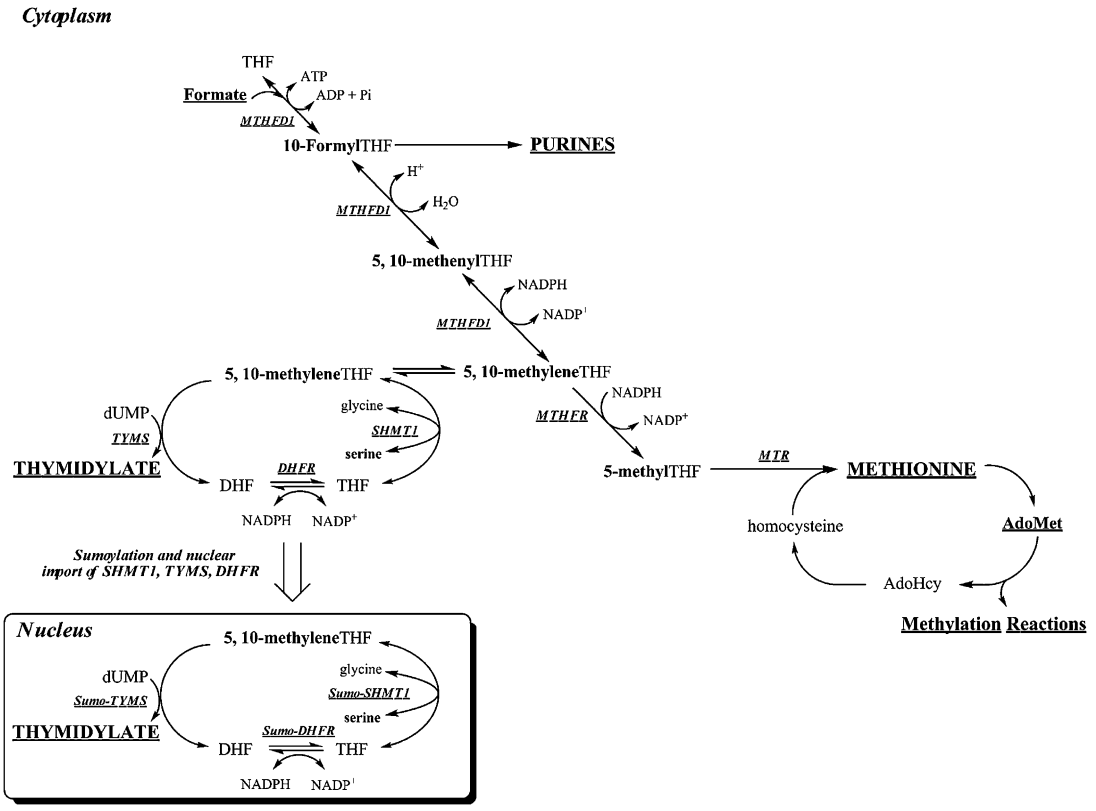

FIGURE 1. Schematic of folate-mediated one-carbon metabolism in the cytoplasm and nucleus. One-carbon metabolism in the cytoplasm is required for the de novo synthesis of purines and thymidylate and for the remethylation of homocysteine to methionine. One-carbon metabolism in the nucleus synthesizes de novo purine and thymidylate (dTMP) from deoxyuridine monophosphate (dUMP) and serine. THF, tetrahydrofolate; MTHFD1, methylenetetrahydrofolate dehydrogenase; MTR, methionine synthase; MTHFR, methylenetetrahydrofolate reductase; SHMT1, cytoplasmic serine hydroxymethyltransferase; TYMS, thymidylate synthase; DHF, dihydrofolate; DHFR, dihydrofolate reductase; AdoMet, *S*-adenosylmethionine; AdoHcy, *S*-adenosylhomocysteine; Sumo, small ubiquitin-like modifier.

midylate synthase (TYMS), dihydrofolate reductase, and serine hydroxymethyltransferase (SHMT) (15) (Figure 1). Two cytoplasmic isoforms of SHMT, SHMT1 and SHMT2α, which are encoded by 2 different genes, undergo small ubiquitin-like modifier (SUMO)–dependent translocation into the nucleus during S-phase to provide dTTP for DNA replication (16, 17). In mice, disruption of *Shmt1* impairs de novo thymidylate biosynthesis (15), resulting in increased uracil misincorporation into DNA (18). *Shmt1* is not essential in mice (18), and *Shmt1* null mice do not develop NTDs when fed a commercial nonpurified rodent diet. However, because human NTDs arise from gene-nutrient interactions, we examined the contribution of *Shmt1* to NTDs during folate and choline deficiency in mice to determine directly if impaired de novo thymidylate biosynthesis increases risk of NTDs.

MATERIALS AND METHODS

Mouse models

Shmt1$^{+/-}$ mice were maintained as heterozygote breeding colonies on either congenic 129/SvEv or C57BL/6 backgrounds (18). Heterozygous C57BL/6J-*Pax3*^{Sp} (*Splotch*) mice were obtained from Jackson Laboratories (Bar Harbor, ME). NTDs were examined in litters harvested from crosses of either 129SvEv-*Shmt1*(N10+) or C57BL/6-*Shmt1*(N10+) mice. To determine the effect of *Shmt1* disruption on NTDs in the *Splotch* mutant, compound *Pax3*,*Shmt1* mutants were obtained by crossing *Shmt1*$^{+/-}$ mice on a mixed C57Bl6/129Sv/EV/Balb/c background to *Pax3*$^{Sp/+}$ mice. F1 compound heterozygotes (*Pax3*$^{Sp/+}$, *Shmt1*$^{+/-}$) were then used for colony breeding. *Pax3*$^{Sp/+}$,*Shmt1*$^{+/-}$ or *Pax3*$^{Sp/+}$,*Shmt1*$^{-/-}$ female mice were then crossed to *Pax3*$^{Sp/+}$, *Shmt1*$^{+/-}$ male mice for timed mating experiments as described below.

Experimental animals and diets

All animal experiments were approved by the Cornell Institutional Animal Care and Use Committee (Cornell University, Ithaca, NY) according to the guidelines of the Animal Welfare Act and all applicable federal and state laws. Mice were maintained on a 12-h light/dark cycle in a temperature-controlled room. For studies investigating *Shmt1* disruption and NTDs, female mice were randomly assigned to receive either an experimental AIN93G diet lacking folate and choline (FCD) or an AIN93G (control) diet (Dyets, Bethlehem, PA) at weaning. Choline was excluded from the experimental diet in addition to folate to increase stress on the homocysteine remethylation cycle and because both dietary folate and choline have been associated with NTD risk. Studies investigating the interaction between *Shmt1* and *Pax3* in compound *Pax3*,*Shmt1* mutants were conducted in mice fed either a commercial nonpurified rodent diet (Harlan, South Easton, MA) or the FCD diet. For all studies, dams were fed the diet from weaning throughout the

breeding period and for the duration of gestation until being killed. Virgin 70- to 120-d-old female mice were housed overnight with males. The following morning, females were examined for the presence of a vaginal plug. Gestational day 0.5 (E0.5) was designated at 0900 the day of the plug. Pregnant females were killed by cervical dislocation between E9.5 and E11.5, and blood was collected by cardiac puncture. Gravid uteri were removed, and all implants and resorption sites were recorded. Embryos were examined for presence of NTDs and measured for crown-rump length. All yolk sacs were collected for subsequent genotyping. Embryos extracted for later use in biochemical assays or for protein extraction were taken at E8.5–10.5 and rapidly frozen in liquid nitrogen followed by storage at −80°C. Embryos examined for morphologic abnormalities were derived at E11.5 and fixed in 10% neutral buffered formalin.

Genotype analysis

Genotyping for the *Splotch* mutation and sex was performed by using established protocols (19, 20). Genotyping for *Shmt1*^{flox} and *Shmt1*$^{+/-}$ alleles was performed by using a previously described protocol (18).

Histology

Embryos were processed for histologic analysis after gross morphologic examination. Tissues were cryoprotected in 30% sucrose in phosphate-buffered saline (PBS), embedded in Optimal Cutting Temperature (Tissue-Tek; Electron Microscopy Sciences, Hatfield, PA) and frozen in isopentane cooled in liquid nitrogen. Thirty-micrometer-thick cryosections were affixed to plus-charged slides and stained with hematoxylin and eosin.

Immunofluorescence

For whole-mount immunofluorescence, E8.0 embryos were fixed in 4% paraformaldehyde and stained by using standard procedures in a block/diluent containing 1% bovine serum albumin and 10% normal donkey serum. Embryos were incubated with sheep anti-SHMT1 antibody (1:50) and visualized with Alexafluor 488-conjugated donkey anti-sheep antibody (1:250; Invitrogen, Carslbad, CA). Paired box gene 3 (PAX3) and SHMT1 double fluorescent immunostaining was performed on transverse 10-μm-thick cryosections of E9.0 embryos by using sheep anti-SHMT1 and mouse anti-PAX3 antibody (1:25; R&D Systems, Minneapolis, MN). Double immunofluorescence was visualized with Alexafluor 488-conjugated donkey anti-mouse antibody (1:100; Invitrogen) and Alexafluor 568-conjugated donkey anti-sheep antibody (1:100; Invitrogen). Sections were counterstained with DAPI (Invitrogen). Immunofluorescent staining was visualized on a Zeiss LSM 510-META confocal microscope (Thornwood, NY) and processed in Volocity 5.2 (Perkin Elmer, Waltham, MA).

Determination of metabolites

Plasma metabolite concentrations were determined as previously described (21, 22). Folate concentrations were quantified by using a *Lactobacillus casei* microbiological assay as previously described (23). Total concentrations of AdoMet and *S*-adenosylhomocysteine (AdoHcy) were measured in frozen mouse embryonic fibroblast (MEF) cell pellets by an established HPLC procedure (24).

Immunoblotting

Western blot analyses were performed in triplicate by using 15–30 μg protein extracted from individual embryos as described elsewhere (18). The primary antibodies were diluted in 5% nonfat skim milk in PBS as follows: monoclonal mouse anti-mouse TYMS antibody (1:2000; Invitrogen), monoclonal mouse anti-mouse GAPDH (glyceraldehyde 3-phosphate dehydrogenase) antibody (1:40,000; Novus Biologicals, Littleton, CO), polyclonal goat anti-mouse PAX3 antibody (1:3000; Santa Cruz Biotechnology, Santa Cruz, CA), polyclonal rabbit anti-mouse actin antibody (1:40,000; Abcam, Cambridge, MA), and polyclonal sheep anti-mouse SHMT1 antibody (1:10,000) (25). Densitometry was performed on autoradiographs by using Image J software (National Institutes of Health, Bethesda, MD).

Generation of mouse embryonic fibroblast cell lines

MEF cell lines were generated from embryos isolated 10–14 d post coitus from crosses of *Pax3*$^{Sp/+}$ mice. MEFs were incubated at 37°C in Defined Minimal Essential Media (Hyclone; Thermo Scientific, Rockford, IL) with 10% fetal bovine serum.

Nucleotide biosynthesis assays

Formate suppression and modified deoxyuridine suppression assays, which measure the relative efficiency of de novo purine and thymidine nucleotide synthesis, respectively, relative to synthesis from nucleotide salvage pathways, was performed as previously described (26, 27). Isotope incorporation into nuclear DNA was quantified by using a Beckman LS6500 scintillation counter (Beckman Coulter, Brea, CA) in dual disintegrations per minute (dpm) mode.

Statistical analyses

Analyses of NTD incidence and embryonic crown-rump length were conducted by using repeated-measured analysis of variance (PROC MIXED or PROC GENMOD, SAS version 9.2; SAS Institute, Cary, NC) and Tukey's honestly significant difference post hoc test. Independent variables included maternal and embryonic *Shmt1* genotype and maternal diet, and litter was considered as a repeated measure. Embryonic *Shmt1* genotype was excluded from the model when assumptions of variance were violated due to the absence of exencephaly observed in *Shmt1*$^{+/+}$ embryos. Embryonic sex was also included in the model, because sex modifies the incidence of exencephaly (8). Analysis of total litter resorptions and implants was conducted by analysis of variance in which litter was considered as the unit of analysis. Independent variables in the model included maternal *Shmt1* genotype and diet. Resorption rate was calculated as the ratio of resorptions to total implants per litter, and log-transformation was applied to normalize the data. Specific comparisons within main effects were assessed by comparisons of least-squares means. Chi-square analyses were used to assess any deviation from expected genotype ratios on the basis of Mendelian inheritance. For cell culture assays and densitometry

measurements, genotype differences were assessed by using a Student's *t* test with a Bonferroni correction for multiple comparisons. Two-tailed *t* tests were used in every case except for the deoxyuridin suppression assay, for which a one-tailed *t* test was used because the direction of the results was expected based on a previous report (10).

RESULTS

Shmt1 disruption sensitizes embryos to exencephaly

We investigated NTD occurrence in mice deficient in *Shmt1* expression in response to maternal folate and choline deficiency to model the gene-nutrient interactions that result in NTDs in humans. We bred $Shmt1^{+/-}$ males to $Shmt1^{+/+}$, $Shmt1^{+/-}$, or $Shmt1^{-/-}$ female mice (congenic 129SvEv or C57BL/6 backgrounds) fed either a modified AIN93G diet (FCD diet) or a control AIN93G diet from weaning and observed a low frequency of exencephaly in both $Shmt1^{+/-}$ or $Shmt1^{-/-}$ embryos (**Figure 2,** A–F; **Tables 1** and **2**). The incidence of NTDs on the 129SvEv background is described below; however, NTDs were also observed, albeit at a lower frequency, on the C57BL/6 background (*see* Supplementary Table 1, A, B, under "Supplemental data" in the online issue). Exencephaly was primarily observed in litters from dams fed the FCD diet ($\chi^2 = 5.91$, $P = 0.0015$), indicating that the NTD phenotype was responsive to maternal folate status, as observed in humans. The frequency of exencephaly was higher for $Shmt1^{-/-}$ littermates (14%; 13 of 92 embryos) as compared with $Shmt1^{+/-}$ embryos (3.2%; 6 of 185 embryos) in litters isolated from dams fed the FCD diet, indicating that complete loss of *Shmt1* expression in the developing embryo was associated with a greater risk of exencephaly when compared with heterozygosity ($\chi^2 = 5.33$, $P = 0.02$). In contrast to the effects of fetal *Shmt1* genotype, maternal *Shmt1* genotype did not significantly influence NTD occurrence, although only one $Shmt1^{+/-}$ embryo with exencephaly (1%; 1 of 101 embryos) was uncovered from crosses involving $Shmt1^{+/+}$ dams fed the FCD diet.

The number of observed $Shmt1^{+/+}$, $Shmt1^{+/-}$, and $Shmt1^{-/-}$ embryos at E11.5 did not deviate from expected values for any of the crosses examined (data not shown). However, we observed that maternal diet ($F = 21.5$, $P < 0.0001$) and embryonic *Shmt1* genotype ($F = 4.45$, $P = 0.01$) significantly affected embryonic growth at E11.5 (Figure 2, G, H). Embryos isolated from dams fed the FCD diet had significantly shorter crown-rump lengths (Figure 2H) as did $Shmt1^{-/-}$ embryos isolated from dams that were fed either diet (Figure 2G). Neither *Shmt1* genotype nor diet significantly affected the weight of female mice at onset of gestation ($P > 0.05$; data not shown) or the number of implantation sites, although the FCD diet resulted in

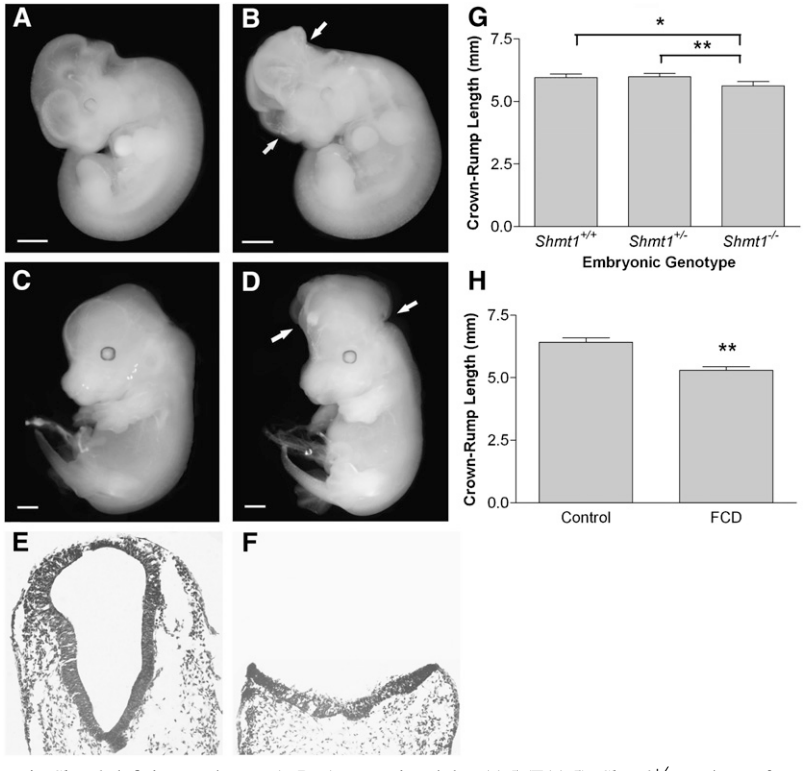

FIGURE 2. Neural tube defects in *Shmt1*-deficient embryos. A, B: At gestational day 11.5 (E11.5), $Shmt1^{+/-}$ embryos from dams fed the diet lacking folate and choline (FCD) exhibited failure of rostral neural tube closure at the midbrain/hindbrain boundary (B). All wild-type littermates (A) were unaffected. Arrows indicate extent of lesions. C, D: At E14.5, affected $Shmt1^{+/-}$ embryos (D) exhibited prominent exencephaly. Wild-type littermates (C) were unaffected. Arrows indicate extent of lesions. E, F: Hematoxylin and eosin–stained transverse sections of the hindbrain region in E10.5 embryos showed complete failure of closure in the hindbrain region in $Shmt1^{+/-}$ embryos (F). Wild-type embryos (E) showed normal closure. G, H: Crown-rump length of embryos derived from crosses of *Shmt1*-deficient mice. Main effects of genotype and diet and the interaction of genotype and diet were determined by mixed-model ANOVA and Tukey's honestly significant difference post hoc test. (G) Crown-rump length as a function of embryonic *Shmt1* genotype. $n = 90$–110 embryos. *Significantly different from $Shmt1^{+/+}$, $P = 0.057$. **Significantly different from $Shmt1^{+/-}$, $P = 0.007$. (H) Crown-rump length as a function of maternal diet. $n = 90$–120 embryos. **Significantly different from control diet, $P \leq 0.01$. The control diet consisted of an experimental feed (AIN93G; Dyets, Bethlehem, PA); FCD refers to an AIN93G diet lacking folate and choline. Scale bars indicate 1 mm.

TABLE 1
Frequency of neural tube defects (NTDs) in *Shmt1*-deficient embryos on a 129/SvEv background as a function of maternal *Shmt1* genotype and diet[1]

Diet and maternal genotype	No. of litters	No. of embryos	No. of NTDs[2]
Control			
Shmt1$^{+/+}$	8	44	0
Shmt1$^{+/-}$	27	149	1 (<1)
Shmt1$^{-/-}$	8	39	0
FCD			
Shmt1$^{+/+}$	19	101	1 (1)
Shmt1$^{+/-}$	36	180	7 (3.9)
Shmt1$^{-/-}$	16	85	11 (13)

[1] Frequency of NTDs observed in litters isolated from crosses of *Shmt1*-deficient mice on a 129/SvEv background on gestational day 11.5. Main effects of maternal *Shmt1* genotype and maternal diet were assessed by using a modified generalized linear model procedure. Maternal diet (χ^2 = 5.91, P = 0.0015) significantly influenced NTD occurrence. The control diet consisted of an experimental feed (AIN93G; Dyets, Bethlehem, PA). FCD, an AIN93G diet lacking folate and choline.
[2] Percentages in parentheses.

TABLE 2
Frequency of neural tube defects (NTDs) in *Shmt1*-deficient embryos on a 129/SvEv background as a function of embryonic *Shmt1* genotype[1]

	Embryonic *Shmt1* genotype[2]		
Maternal *Shmt1* genotype	*Shmt1*$^{+/+}$	*Shmt1*$^{+/-}$	*Shmt1*$^{-/-}$
Shmt1$^{+/+}$			
No. of NTDs	0	1 (1.8)	—
No. of embryos	46	55	—
Shmt1$^{+/-}$			
No. of NTDs	0	3 (3.4)	4 (8.2)
No. of embryos	43	88	49
Shmt1$^{-/-}$			
No. of NTDs	—	2 (4.8)	9 (21)
No. of embryos	—	42	43

[1] Frequency of NTDs observed in gestational day 11.5 embryos isolated from crosses of *Shmt1*-deficient mice on a 129/SvEv background fed the AIN93G diet lacking folate and choline (FCD diet; Dyets, Bethlehem, PA). The effect of embryonic *Shmt1* genotype was assessed by using a modified generalized linear model procedure. The frequency of exencephaly was higher for *Shmt1*$^{-/-}$ littermates (14%; 13 of 92 embryos) than for *Shmt1*$^{+/-}$ embryos in litters isolated from dams fed the FCD diet (3.2%; 6 of 185 embryos) (χ^2 = 5.33, P = 0.02).
[2] Percentages in parentheses.

significantly more resorptions per litter (22.4% with the FCD diet compared with. 9.7% with the control diet; F = 7.52, P = 0.0094).

Maternal *Shmt1* disruption does not influence markers of folate status

To gain further insight into the metabolic mechanisms underlying NTD pathogenesis, we investigated the effect of diet and *Shmt1* genotype on biomarkers of folate status in pregnant dams. Maternal *Shmt1* genotype did not influence red blood cell (RBC) folate concentrations in pregnant dams receiving the FCD diet [*Shmt1*$^{+/+}$ (11 fmol/μg) compared with *Shmt1*$^{+/-}$ (13 fmol/μg) compared with *Shmt1*$^{-/-}$ (6.5 fmol/μg); $P > 0.05$], whereas the FCD diet resulted in a significant reduction in RBC folate concentrations (F = 2637, $P < 0.0001$; *see* Supplementary Figure 1 under "Supplemental data" in the online issue). RBC folate concentrations were reduced by ≈80% in female mice fed the FCD diet compared with the control diet. Similarly, maternal *Shmt1* genotype did not influence plasma homocysteine concentrations or the concentrations of several metabolites associated with homocysteine remethylation and metabolism (*see* Supplementary Table 2 under "Supplemental data" in the online issue). The FCD diet resulted in plasma homocysteine concentrations that were elevated >3-fold relative to concentrations observed with the control diet (49 ± 7.1 compared with 15 ± 3.5 μmol/L). The FCD diet also significantly affected concentrations of all metabolites associated with homocysteine remethylation (*see* Supplementary Table 2 under "Supplemental data" in the online issue). These data are consistent with an effect of maternal diet, but not maternal *Shmt1* genotype, on NTD occurrence.

Metabolic disruption of folate-mediated OCM in *Splotch* MEFs

To assess whether a common mechanism underlies folate-responsive NTDs in the *Splotch* mutant, we examined the metabolic phenotype of *Pax3*$^{Sp/Sp}$ MEFs generated from *Splotch* matings. Consistent with a previous report (10), we observed a trend toward an impairment in de novo thymidylate biosynthesis in *Pax3*$^{Sp/Sp}$ MEF lines (P = 0.1; **Figure 3**A). Surprisingly, *Splotch* MEF lines also exhibited gene-dosage-dependent impairments in de novo purine biosynthesis (Figure 3B). *Pax3*$^{Sp/Sp}$ lines exhibited significantly reduced rates of de novo purine biosynthesis compared with *Pax3*$^{+/+}$ lines (P = 0.04). The relative ratio of AdoMet to AdoHcy, which serves as an indicator of the cellular methylation potential, increased in a gene-dosage–dependent manner in response to the *Splotch* mutation, although only the comparison between *Pax3*$^{Sp/Sp}$ and *Pax3*$^{+/+}$ lines was significant (P = 0.004; Figure 3C). These data support the hypothesis that impairments in nucleotide biosynthesis underlie NTD pathogenesis in folate-responsive NTDs.

Shmt1 and *Pax3* interact in neural tube closure

Because disruption of either *Shmt1* or *Pax3* impairs thymidylate biosynthesis, we reasoned that *Shmt1* and *Tyms* expression might be altered in *Splotch* embryos. We examined SHMT1 concentrations in *Splotch* embryos and observed increased SHMT1 protein concentrations in *Pax3*$^{Sp/+}$ (P = 0.009) and *Pax3*$^{Sp/Sp}$ ($P < 0.0001$) embryos relative to *Pax3*$^{+/+}$ embryos at E10.5 (**Figure 4**A). However, SHMT1 was not misexpressed in *Splotch* embryos, because whole-mount immunofluorescence did not reveal altered domains of expression (*see* Supplementary Figure 2 under "Supplemental data" in the online issue). We also observed reduced TYMS protein concentrations in response to the *Splotch* mutation in both *Pax3*$^{Sp/+}$ (P = 0.04) and *Pax3*$^{Sp/Sp}$ (P = 0.02) embryos (Figure 4B), which is consistent with the observation of impaired thymidylate biosynthesis in *Splotch* MEFs. Examination of *Shmt1* and *Tyms* message levels by real-time polymerase chain reaction did not reveal any genotype differences (data not shown), indicating that the *Splotch* mutation affects SHMT1 and TYMS protein concentrations

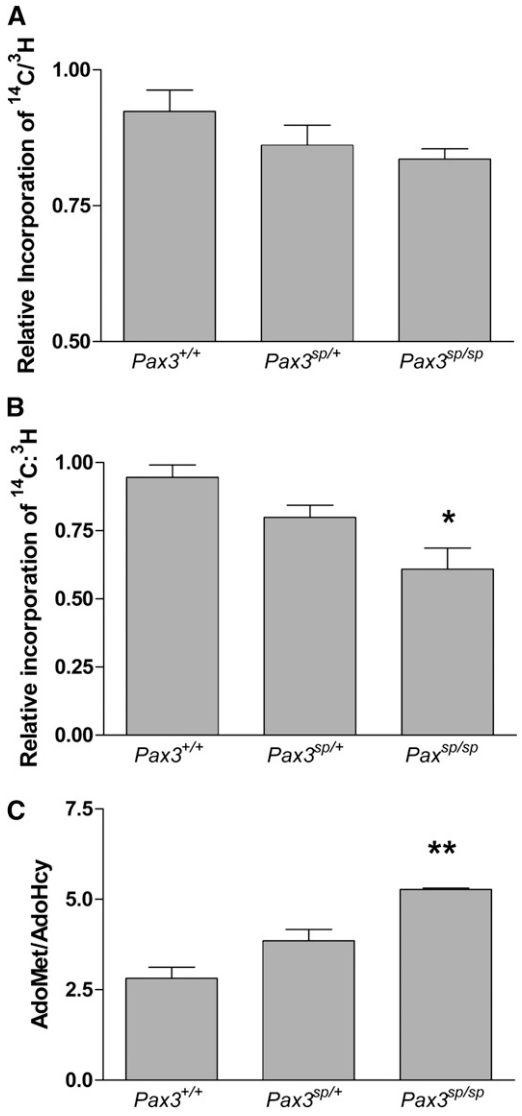

FIGURE 3. Metabolic phenotype of the *Splotch* mutant. A–C: Metabolic phenotype in *Splotch* mouse embryonic fibroblasts (MEFs). $Pax3^{+/+}$, $Pax3^{Sp/+}$, and $Pax3^{Sp/Sp}$ MEF cells were cultured to confluency in α-minimal essential medium supplemented with ^{14}C-deoxyuridine monophosphate (^{14}C-dUMP) and ^{3}H-thymidine or ^{14}C-formate and ^{3}H-hypoxanthine. Efficiency of de novo thymidylate biosynthesis (A) was determined by the relative enrichment of ^{14}C-dUMP (10 μmol/L)/^{3}H-thymidine (500 nmol) in nuclear DNA, and the efficiency of de novo purine biosynthesis (B) was determined by the relative enrichment of ^{14}C-formate (20 μmol/L)/^{3}H-hypoxanthine (2 nmol) in nuclear DNA. All values represent the average of triplicate measures of 3 different cell lines per genotype. (C) The relative ratio of *S*-adenosylmethionine (AdoMet) to *S*-adenosylhomocysteine (AdoHcy) was measured in $Pax3^{+/+}$, $Pax3^{Sp/+}$, and $Pax3^{Sp/Sp}$ MEF lines. n = 2–3 lines per genotype. Results for all experiments are shown as means ± SDs. All genotype differences were determined by using a Student's t test. *Significantly different from $Pax3^{+/+}$, $P \leq 0.05$. **Significantly different from $Pax3^{+/+}$, $P < 0.01$.

posttranscriptionally. Interestingly, PAX3 and SHMT1 protein concentrations appear to be mutually regulated and compensatory, because we also observed increased PAX3 protein concentrations in $Shmt1^{+/-}$ (P = 0.08) and $Shmt1^{-/-}$ (P = 0.09) embryos (Figure 4C). Disruption of *Shmt1* also resulted in reduced TYMS protein concentrations in $Shmt1^{-/-}$ embryos (Figure 4D). These data suggest that mutual regulation of PAX3 and SHMT1 protein concentrations may compensate for impairments in de novo thymidylate biosynthesis.

SHMT1 and PAX3 colocalize within the neural tube

Because SHMT1 and PAX3 protein concentrations, but not mRNA concentrations, were mutually regulated in *Splotch* mutants and SHMT1-deficient embryos, colocalization of SHMT1 and PAX3 in the neural tube of wild-type embryos was determined by immunofluorescence. As described previously (28), strong PAX3 immunoreactivity was observed within the dorsal neural tube, with the ventral border of expression delimited by the sulcus limitans (Figure 4, E–H). Neuroepithelial expression was observed from the level of the diencephalon through the caudal end of the neural tube (Figure 4, E–G). Strong PAX3 immunoreactivity was also observed in neural crest. SHMT1 and PAX3 expression colocalized within the neuroepithelium and the neural crest, primarily at the level of the hindbrain/cervical flexure (Figure 4E). Cytoplasmic expression of SHMT1 was observed in a longitudinal band located dorsal to the sulcus limitans. Overlapping domains of PAX3 and SHMT1 expression were observed in this region as well as in the migrating neural crest (Figure 4F). Some limited coexpression was also observed in more caudal regions of the neural tube (Figure 4G). The observed coexpression of SHMT1 and PAX3 within the neural tube further suggests that these 2 proteins are coexpressed during neural tube closure.

Shmt1 disruption exacerbates the NTD phenotype in *Splotch* embryos

To test for an interaction at the level of metabolism between PAX3 and SHMT1 during neural tube closure, we crossed the $Shmt1^{-/-}$ mice to the *Splotch* mouse model and determined whether aggravated impairments in de novo thymidylate biosynthesis in compound mutants would exacerbate NTDs. *Shmt1* disruption increased the frequency of more severe lesions in homozygous *Splotch* embryos (**Figure 5**A), which included lesions in both the cranial and spinal regions. $Pax3^{Sp/Sp}$,$Shmt1^{+/-}$ and $Pax3^{Sp/Sp}$,$Shmt1^{-/-}$ embryos had significantly higher incidence of combined spina bifida and exencephaly (46% and 66%, respectively) compared with embryos isolated from crosses involving the *Splotch* mutation alone (22%; P = 0.04 and 0.001, respectively), whereas the incidence of combined lesions in $Pax3^{Sp/Sp}$,$Shmt1^{+/+}$ embryos isolated from compound mutant crosses (22%) did not differ from the effects of the *Splotch* mutation alone ($P > 0.95$). In addition to increasing the severity of NTDs observed in $Pax3^{Sp/Sp}$ embryos, *Shmt1* disruption also resulted in instances of $Pax3^{Sp/+}$ and $Pax3^{+/+}$ littermates with spina bifida or exencephaly under folate-replete conditions (*see* Supplementary Table 3 under "Supplemental data" in the online issue; Figure 5, B–E). $Pax3^{Sp/+}$ and $Pax3^{+/+}$ embryos with NTDs were either $Shmt1^{+/-}$ or $Shmt1^{-/-}$ in all cases. Approximately 3–5% of $Pax3^{+/+}$ and $Pax3^{Sp/+}$ embryos from compound mutant crosses that were fed a commercial nonpurified rodent diet displayed NTDs. In most cases, the lesion observed was exencephaly, but isolated spina bifida was also observed in a few cases (Figure 5, B, C); the severity of these lesions was comparable to that observed in $Pax3^{Sp/Sp}$ embryos. Whereas lesions induced by *Shmt1* disruption alone were confined to the cranial region, embryonic *Shmt1* disruption resulted in spina bifida in response to either embryonic or maternal heterozygosity for the *Splotch* mutation. Furthermore, embryonic or maternal *Pax3* heterozygosity was sufficient to induce spina bifida or exencephaly

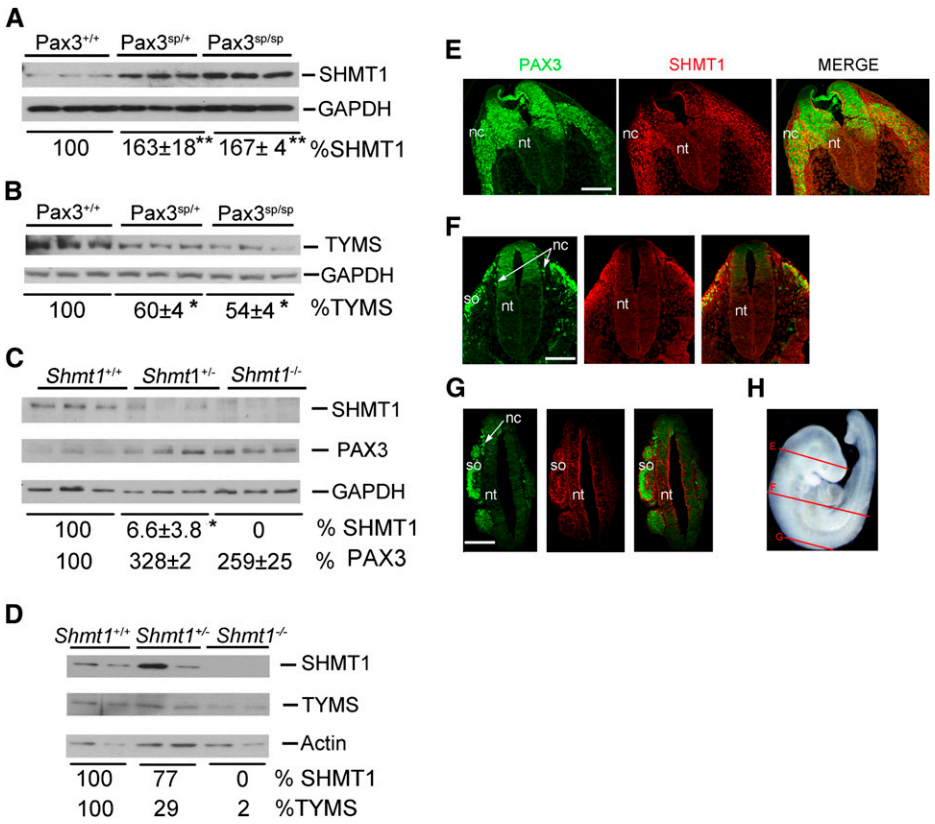

FIGURE 4. Serine hydroxymethyltransferase (SHMT1) and paired box gene 3 (PAX3) interact in the neural tube. A, B: Protein extracts from gestational day 10.5 (E10.5) embryos isolated from *Splotch* crosses fed the commercial diet were analyzed by Western blot with a polyclonal anti-SHMT1 antibody (A) and a monoclonal anti-thymidylate synthase (anti-TYMS) antibody (B). Glyceraldehyde 3-phosphate dehydrogenase (GAPDH) was probed with a polyclonal antibody to verify equal loading in both experiments. Relative concentrations of SHMT1 (A) and TYMS (B) were quantified by densitometry with the use of GAPDH as a control. Genotype differences were analyzed by Student's *t* test with Bonferroni correction ($n = 3$). Both SHMT1 and TYMS protein concentrations were responsive to the *Splotch* mutation. *Significantly different from $Pax3^{+/+}$, $P < 0.05$. **Significantly different from $Pax3^{+/+}$, $P \leq 0.01$. C, D: Protein extracts from E8.5 embryos isolated from crosses of $Shmt1^{+/-}$ dams fed the AIN93G diet lacking folate and choline (FCD diet; Dyets, Bethlehem, PA) were analyzed by Western blot with the use of a polyclonal antibody to PAX3 (C) and TYMS (D). GAPDH and actin were probed to verify equal loading. Relative concentrations of PAX3, SHMT1, and TYMS were quantified by densitometry with the use of GAPDH (C) or actin (D) as a control. Genotype differences for panel C were analyzed by Student's *t* test with Bonferroni correction ($n = 3$). Both PAX3 and TYMS protein concentrations were responsive to *Shmt1* disruption. *Significantly different from $Pax3^{+/+}$, $P < 0.05$. E–G: Confocal fluorescent immunohistologic localization of SHMT1 (red) and PAX3 (green) protein in transverse sections at the cephalic level (E), midtrunk (F), and lower trunk (G) in a wild-type E9.0 embryo. Locations of sections are shown in panel H. Scale bars represent 90 μmol/L. nc, neural crest; nt, neural tube; so, somite.

in $Shmt1^{+/-}$ and $Shmt1^{-/-}$ embryos in the absence of dietary folate and choline deficiency. Thus, *Shmt1* disruption at both embryonic and maternal levels increased the frequency of exencephaly in *Splotch* embryos, whereas the only instances of spina bifida observed in $Shmt1^{+/-}$ or $Shmt1^{-/-}$ embryos occurred in litters derived from $Pax3^{Sp/+}$ dams.

Because NTDs in SHMT1-deficient embryos were sensitive to maternal folate and choline status, we examined the effect of maternal folate and choline deficiency on NTD extent and frequency in litters isolated from compound *Pax3*,*Shmt1* mutants fed the FCD diet. Impaired maternal folate and choline status both exacerbated and increased the frequency of lesions observed in response to combined *Pax3* and *Shmt1* disruption. Occasional cases of craniorachischisis were observed in $Pax3^{Sp/+}$, $Shmt1^{-/-}$ and $Pax3^{Sp/Sp}$, $Shmt1^{-/-}$ embryos (Figure 5, F, G). To our knowledge, craniorachischisis has not been reported previously in response to the *Splotch* mutation alone. Furthermore, the frequency of NTDs observed in $Pax3^{Sp/+}$ littermates rose from 3–5% to 11–14% in response to dietary folate and choline deficiency in compound *Pax3,Shmt1* mutant crosses (*see* Supplementary Table 4 under "Supplemental data" in the online issue). The majority of NTDs in $Pax3^{+/+}$ and $Pax3^{Sp/+}$ littermates were confined to the cranial region.

DISCUSSION

SHMT1 is the first folate-dependent enzyme shown to sensitize mice to NTDs by disrupting folate metabolism, and the results directly implicate impaired thymidylate synthesis and *Shmt1* in the etiology of folate-responsive NTDs. The *Shmt1* mouse model recapitulates the gene-diet interactions that confer NTD risk in humans, with embryonic *Shmt1* disruption essential for NTD pathogenesis, but NTD penetrance increased by maternal folate and choline deficiency. In the cytoplasm, SHMT1 regulates the partitioning of one-carbon units between thymidylate biosynthesis and homocysteine remethylation (24), whereas in the nucleus SHMT1 is a source of folate-activated one-carbon units for thymidylate synthesis (16). Consequently, de novo thymidylate biosynthesis is impaired in the nuclei of *Shmt1* null mice (15), and decreased *Shmt1* expression increases

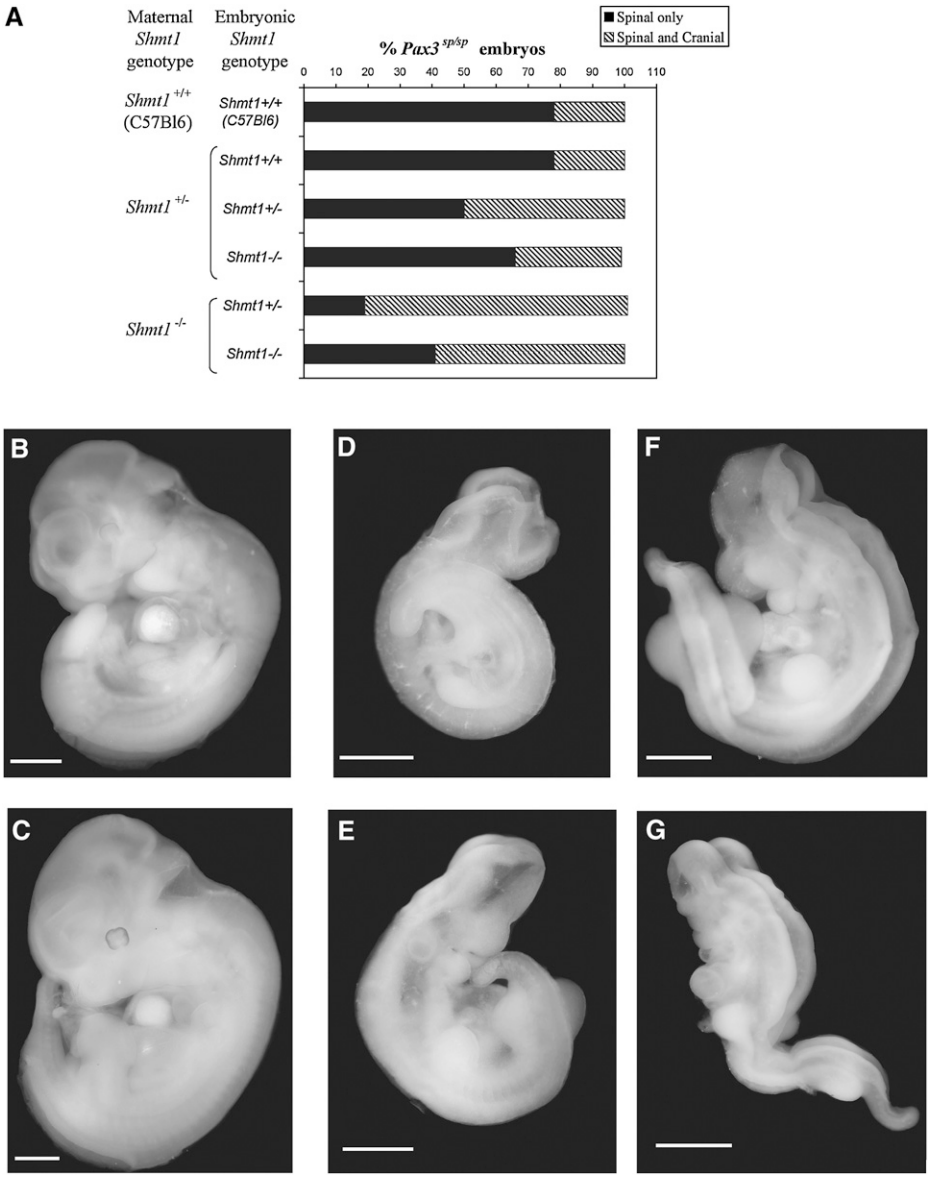

FIGURE 5. *Shmt1* disruption exacerbates neural tube defects in *Splotch* mutants. A: Incidence of spinal and combined cranial + spinal lesions in $Pax3^{Sp/Sp}$ embryos isolated from compound mutant crosses (*Pax3*,*Shmt1*) and C57BL/6J-$Pax3^{Sp}$ crosses fed a commercial nonpurified rodent diet. B, C: Spina bifida in $Pax3^{+/+}$,$Shmt1^{+/-}$ (B) and $Pax3^{Sp/+}$,$Shmt1^{+/-}$ (C) embryos derived from compound mutant crosses fed a commercial nonpurified rodent diet. D, E: Exencephaly in $Pax3^{+/+}$,$Shmt1^{+/-}$ (D) and $Pax3^{Sp/+}$,$Shmt1^{+/-}$ (E) embryos derived from compound mutant crosses fed a commercial nonpurified rodent diet. F, G: Craniorachiscisis in $Pax^{Sp/+}$,$Shmt1^{-/-}$ (F) and $Pax3^{Sp/Sp}$,$Shmt1^{-/-}$ (G) embryos derived from compound mutant crosses fed the AIN93G diet lacking folate and choline (Dyets, Bethlehem, PA). Scale bars represent 1 mm.

uracil misincorporation into nuclear DNA in livers of $Shmt1^{+/-}$ mice (18). Although impairment in de novo thymidylate biosynthesis has previously been implicated in folate-responsive NTDs in the $Pax3^{Sp}$ mutant (10), as well as in NTD-affected human fetuses (29), this is the first direct evidence that disruption of folate- and SHMT1-dependent thymidylate biosynthesis underlies NTD pathogenesis. Impairments in de novo thymidylate biosynthesis may disrupt neural tube closure by reducing proliferative capacity or by increasing genomic instability via misincorporation of uracil into DNA (30). Decreased crown-rump lengths observed in $Shmt1^{-/-}$ embryos may reflect reduced proliferative capacity. Genome instability produced via non–folate-dependent pathways can also cause NTDs in mice (31, 32).

Shmt1 and *Pax3* disruption interact epistatically to increase the frequency and severity of NTDs in $Pax3^{Sp/Sp}$ embryos and cause NTDs in $Pax3^{Sp/+}$ and $Pax3^{+/+}$ embryos in the absence of folate deficiency. To our knowledge, these studies are the first to show that the folate-responsive *Splotch* mutation impairs de novo purine biosynthesis and that *Pax3* disruption decreases TYMS concentrations in *Splotch* embryos. Similarly, *Shmt1* disruption has recently been shown to impair de novo thymidylate biosynthesis in isolated nuclei (15); *Shmt1* disruption also decreased TYMS enzyme concentrations in neurulation-stage embryos in the present study. Thus, the demonstrated effects of *Shmt1* and *Pax3* disruption on de novo nucleotide biosynthesis and the synergistic effect of *Shmt1* and *Pax3* disruption on NTD occurrence and severity provide further evidence that impaired

nucleotide biosynthesis underlies NTD pathogenesis. Of interest, PAX3 and SHMT1 protein concentrations appear to be mutually regulated and compensatory. PAX3 and SHMT1 are present during neurulation in the same cells within the dorsal neural tube and migrating neural crest at the level of the hindbrain/cephalic flexure, which is affected in exencephalic embryos. *Shmt1* disruption increased PAX3 protein concentrations, and SHMT1 protein concentrations were similarly elevated in response to *Pax3* disruption. Increased SHMT1 protein concentrations in *Splotch* embryos may compensate partially for reduced TYMS protein concentrations by increasing the concentration of methylenetetrahydrofolate, the required cofactor for TYMS. Similarly, increased concentrations of PAX3, a nuclear transcription factor, observed in response to *Shmt1* disruption in embryos, may function to elevate TYMS concentrations to increase rates of thymidylate biosynthesis. However, the mechanism by which *Pax3* influences de novo thymidylate biosynthesis remains to be determined. Although TYMS protein concentrations were depressed in *Splotch* embryos, *Tyms* message levels were unchanged, indicating that *Tyms* is not a direct downstream transcriptional target of *Pax3*. The regulation of TYMS protein concentrations occurs at many levels including translational autoregulation (33). Furthermore, TYMS protein concentrations do not necessarily reflect or predict de novo thymidylate biosynthesis capacity; nuclei isolated from *Shmt1*$^{-/-}$ mice exhibit severely impaired de novo thymidylate biosynthesis despite increased TYMS protein concentrations (15). Although the molecular mechanisms underlying the interactions between PAX3, SHMT1, and TYMS remain to be established, these interactions appear to afford some protection against NTDs by ensuring thymidylate biosynthesis capacity. When this protective mechanism is disrupted in compound *Pax3*,*Shmt1* mutants, the NTD phenotype is exacerbated.

In this study, *Pax3* disruption in MEFs was shown to impair de novo purine biosynthesis, and the magnitude of the impairment was greater than that observed for thymidylate biosynthesis. This observation may account for the disparity in NTD phenotype between the *Pax3* and *Shmt1* NTD models; *Shmt1* disruption alone is associated only with exencephaly, whereas *Pax3* deficiency causes 100% penetrant spina bifida and low-frequency exencephaly. Furthermore, *Shmt1* deficiency at both maternal and embryonic levels increased the frequency of exencephaly in *Splotch* embryos, whereas the only instances of spina bifida observed in *Shmt1*$^{+/-}$ or *Shmt1*$^{-/-}$ embryos occurred in litters derived from *Pax3*$^{Sp/+}$ dams. Further aggravation of impaired nucleotide biosynthesis in compound *Pax3*, *Shmt1* mutants by maternal dietary folate restriction resulted in some instances of complete failure of neural tube closure. These data suggest that, in mice, impaired purine biosynthesis at either the maternal or fetal level increases risk of spina bifida, whereas impairments in maternal and fetal thymidylate biosynthesis can cause exencephaly. Maternal supplementation with thymidine has been shown to prevent some proportion of NTDs in *Splotch* embryos, a majority of which include the combined spinal and cranial lesion (9, 10). Thus, thymidine may be a maternally derived factor that prevents NTDs.

We have shown that *Shmt1* heterozygosity is sufficient to induce NTDs in mice, and therefore factors that affect *Shmt1* expression are candidate risk factors for NTDs in humans. Cellular SHMT1 activity and concentrations vary over a wide range. *Shmt1* expression is regulated by zinc (34), retinoic acid (35), heavy-chain ferritin (27, 36), and c-Myc (37). Whereas most screens for human NTD candidate genes have focused on the identification of gene variants that encode folate-dependent enzymes with altered function, this study shows that relatively modest changes in SHMT1 concenetrations confer increased NTD risk. Because SHMT1 and TYMS are regulated robustly at the level of translation, this may account for the paucity of human NTD candidate genes in the folate metabolic network identified to date. Indeed, although a limited number of human studies have yet to identify *Shmt1* variants as risk factors for NTDs, further investigation of factors that modulate SHMT1 expression and thymidylate biosynthesis capacity is warranted.

We thank Sylvia Allen, Rachel Slater, Dina Diskina, and Donald Anderson for technical assistance.

The authors' responsibilities were as follows—AEB: study conception and design, data collection and analysis, and manuscript preparation, editing, and revision; EVA, CAP, SC, SPS, and RHA: data collection; DMN: study design and manuscript preparation and editing; and PJS: study conception and design and manuscript editing and revision. There were no conflicts of interest for any of the authors.

REFERENCES

1. International Clearinghouse for Birth Defects Monitoring Systems. World atlas of birth defects. 2 ed. Geneva, Switzerland: World Health Organization, 2003.
2. Kirke PN, Molloy AM, Daly LE, Burke H, Weir DG, Scott JM. Maternal plasma folate and vitamin B12 are independent risk factors for neural tube defects. Q J Med 1993;86:703–8.
3. Relton CL, Wilding CS, Laffling AJ, et al. Low erythrocyte folate status and polymorphic variation in folate-related genes are associated with risk of neural tube defect pregnancy. Mol Genet Metab 2004;81:273–81.
4. Christensen B, Arbour L, Tran P, et al. Genetic polymorphisms in methylenetetrahydrofolate reductase and methionine synthase, folate levels in red blood cells, and risk of neural tube defects. Am J Med Genet 1999;84:151–7.
5. Czeizel AE, Dudas I. Prevention of the first occurrence of neural-tube defects by periconceptional vitamin supplementation. N Engl J Med 1992;327:1832–5.
6. Medical Research Council. Prevention of neural tube defects: results of the Medical Research Council Vitamin Study. MRC Vitamin Study Research Group. Lancet 1991;338:131–7.
7. Stover PJ. Physiology of folate and vitamin B12 in health and disease. Nutr Rev 2004;62:S3–12; discussion: S13.
8. Harris MJ, Juriloff DM. Mouse mutants with neural tube closure defects and their role in understanding human neural tube defects. Birth Defects Res A Clin Mol Teratol 2007;79:187–210.
9. Wlodarczyk BJ, Tang LS, Triplett A, Aleman F, Finnell RH. Spontaneous neural tube defects in splotch mice supplemented with selected micronutrients. Toxicol Appl Pharmacol 2005;213(1):55–63.
10. Fleming A, Copp AJ. Embryonic folate metabolism and mouse neural tube defects. Science 1998;280:2107–9.
11. Barbera JP, Rodriguez TA, Greene ND, et al. Folic acid prevents exencephaly in Cited2 deficient mice. Hum Mol Genet 2002;11:283–93.
12. Carter M, Ulrich S, Oofuji Y, Williams DA, Ross ME. Crooked tail (Cd) models human folate-responsive neural tube defects. Hum Mol Genet 1999;8:2199–204.
13. Trembath D, Sherbondy AL, Vandyke DC, et al. Analysis of select folate pathway genes, PAX3, and human T in a Midwestern neural tube defect population. Teratology 1999;59:331–41.
14. Lu W, Zhu H, Wen S, et al. Screening for novel PAX3 polymorphisms and risks of spina bifida. Birth Defects Res A Clin Mol Teratol 2007; 79:45–9.
15. Anderson DD, Stover PJ. SHMT1 and SHMT2 are functionally redundant in nuclear de novo thymidylate biosynthesis. PLoS ONE 2009; 4:e5839.
16. Anderson DD, Woeller CF, Stover PJ. Small ubiquitin-like modifier-1 (SUMO-1) modification of thymidylate synthase and dihydrofolate reductase. Clin Chem Lab Med 2007;45:1760–3.

17. Woeller CF, Anderson DD, Szebenyi DM, Stover PJ. Evidence for small ubiquitin-like modifier-dependent nuclear import of the thymidylate biosynthesis pathway. J Biol Chem 2007;282:17623–31.
18. MacFarlane AJ, Liu X, Perry CA, et al. Cytoplasmic serine hydroxymethyltransferase regulates the metabolic partitioning of methylenetetrahydrofolate but is not essential in mice. J Biol Chem 2008;283: 25846–53.
19. Machado AF, Zimmerman EF, Hovland DN Jr, Weiss R, Collins MD. Diabetic embryopathy in C57BL/6J mice: altered fetal sex ratio and impact of the splotch allele. Diabetes 2001;50:1193–9.
20. McClive PJ, Sinclair AH. Rapid DNA extraction and PCR-sexing of mouse embryos. Mol Reprod Dev 2001;60:225–6.
21. Stabler SP, Lindenbaum J, Savage DG, Allen RH. Elevation of serum cystathionine levels in patients with cobalamin and folate deficiency. Blood 1993;81:3404–13.
22. Allen RH, Stabler SP, Savage DG, Lindenbaum J. Elevation of 2-methylcitric acid I and II levels in serum, urine, and cerebrospinal fluid of patients with cobalamin deficiency. Metabolism 1993;42: 978–88.
23. Suh JR, Oppenheim EW, Girgis S, Stover PJ. Purification and properties of a folate-catabolizing enzyme. J Biol Chem 2000;275: 35646–55.
24. Herbig K, Chiang EP, Lee LR, Hills J, Shane B, Stover PJ. Cytoplasmic serine hydroxymethyltransferase mediates competition between folate-dependent deoxyribonucleotide and S-adenosylmethionine biosyntheses. J Biol Chem 2002;277:38381–9.
25. Liu X, Szebenyi DM, Anguera MC, Thiel DJ, Stover PJ. Lack of catalytic activity of a murine mRNA cytoplasmic serine hydroxymethyltransferase splice variant: evidence against alternative splicing as a regulatory mechanism. Biochemistry 2001;40:4932–9.
26. Field MS, Szebenyi DM, Stover PJ. Regulation of de novo purine biosynthesis by methenyltetrahydrofolate synthetase in neuroblastoma. J Biol Chem 2006;281:4215–21.
27. Oppenheim EW, Adelman C, Liu X, Stover PJ. Heavy chain ferritin enhances serine hydroxymethyltransferase expression and de novo thymidine biosynthesis. J Biol Chem 2001;276:19855–61.
28. Goulding MD, Chalepakis G, Deutsch U, Erselius JR, Gruss P. Pax-3, a novel murine DNA binding protein expressed during early neurogenesis. EMBO J 1991;10:1135–47.
29. Dunlevy LP, Chitty LS, Burren KA, et al. Abnormal folate metabolism in foetuses affected by neural tube defects. Brain 2007;130:1043–9.
30. Blount BC, Mack MM, Wehr CM, et al. Folate deficiency causes uracil misincorporation into human DNA and chromosome breakage: implications for cancer and neuronal damage. Proc Natl Acad Sci USA 1997;94:3290–5.
31. Hollander MC, Sheikh MS, Bulavin DV, et al. Genomic instability in Gadd45a-deficient mice. Nat Genet 1999;23:176–84.
32. Herrera E, Samper E, Blasco MA. Telomere shortening in mTR−/− embryos is associated with failure to close the neural tube. EMBO J 1999;18:1172–81.
33. Tai N, Schmitz JC, Liu J, et al. Translational autoregulation of thymidylate synthase and dihydrofolate reductase. Front Biosci 2004;9: 2521–6.
34. Perry C, Sastry R, Nasrallah IM, Stover PJ. Mimosine attenuates serine hydroxymethyltransferase transcription by chelating zinc: implications for inhibition of DNA replication. J Biol Chem 2005;280:396–400.
35. Nakshatri H, Bouillet P, Bhat-Nakshatri P, Chambon P. Isolation of retinoic acid-repressed genes from P19 embryonal carcinoma cells. Gene 1996;174:79–84.
36. Woeller CF, Fox JT, Perry C, Stover PJ. A ferritin-responsive internal ribosome entry site regulates folate metabolism. J Biol Chem 2007; 282:29927–35.
37. Nikiforov MA, Chandriani S, O'Connell B, et al. A functional screen for Myc-responsive genes reveals serine hydroxymethyltransferase, a major source of the one-carbon unit for cell metabolism. Mol Cell Biol 2002;22:5793–800.